Kinetics and mechanism of cell membrane electrofusion

Iziaslav G. Abidor*‡ and Arthur E. Sowers‡§

*Department of Bioelectrochemistry, A. N. Frumkin Institute of Electrochemistry, Russian Academy of Sciences, 117071 Moscow, Russia; ‡Cell Biology Laboratory, Jerome H. Holland Laboratory for the Biomedical Sciences, Rockville, Maryland 20855; and §Department of Biophysics, School of Medicine, University of Maryland at Baltimore, Baltimore, Maryland 21201

ABSTRACT A new quantitative approach to study cell membrane electrofusion has been developed. Erythrocyte ghosts were brought into close contact using dielectrophoresis and then treated with one square or exponentially decaying fusogenic pulse. Individual fusion events were followed by lateral diffusion of the fluorescent lipid analogue 1,1′-dihexadecyl-3,3,3′,3′-tetramethylindocarbocyanine perchlorate (DiI) from originally labeled to unlabeled adjacent ghosts. It was found that ghost fusion can be described as a first-order rate process with corresponding rate constants: a true fusion rate constant, k_f, for the square waveform pulse and an effective fusion rate constant, k_{ef}, for the exponential pulse. Compared with the fusion yield, the fusion rate constants are more fundamental characteristics of the fusion process and have implications for its mechanism. Values of k_f for rabbit and human erythrocyte ghosts were obtained at different electric field strength and temperatures. Arrhenius k_f plots revealed that the activation energy of ghost electrofusion is in the range of 6–10 kT. Measurements were also made with the rabbit erythrocyte ghosts exposed to 42°C for 10 min (to disrupt the spectrin network) or 0.1–1.0 mM uranyl acetate (to stabilize the bilayer lipid matrix of membranes). A correlation between the dependence of the fusion and previously published pore-formation rate constants for all experimental conditions suggests that the cell membrane electrofusion process involve pores formed during reversible electrical breakdown. A statistical analysis of fusion products (*a*) further supports the idea that electrofusion is a stochastic process and (*b*) shows that the probability of ghost electrofusion is independent of the presence of DiI as a label as well as the number of fused ghosts.

INTRODUCTION

The molecular mechanisms by which cell membranes fuse with each other in nature or in vitro are poorly understood. Unique insight into at least some aspects of this phenomenon may be possible through the induction of cell membrane fusion with an electric field pulse, a protocol often referred to as electrofusion (Senda et al., 1979; Pilwat et al., 1981). As a fusogen the electric pulse is (*a*) relatively independent of the type of cells, (*b*) nonchemical, (*c*) transient, and (*d*) available to synchronize other electrical or optical data recording devices. The electrofusion protocol normally includes two steps: bringing cell membranes into contact and treatment of the membranes with at least one electric pulse to initiate the fusion process (Abidor et al., 1989; Sowers, 1989*a*; Sowers, 1992). Dielectrophoresis (Pohl, 1978), a phenomenon in which a weak alternating electric field causes cells to come into contact through "pearl chain" formation, has additional features: it is a relatively mild, reversible, and nonchemical effect. Thus the fusogenic electric pulse, the method of inducing cell–cell contact, and the aqueous medium can all be manipulated independently of one another in studies of membrane fusion mechanisms.

Although electrofusion has experienced increasing use in biotechnology (Neumann et al., 1989), its mechanism is still poorly understood. Therefore, elucidating the mechanism of electrofusion is a problem of both practical and theoretical importance.

Electrofusion has now been extensively characterized and the protocols have been validated using erythrocyte ghosts as the model membrane system (Sowers, 1989*a* for review). Based on this, a new quantitative approach to electrofusion was developed in this paper.

Address correspondence to Dr. Sowers, Department of Biophysics, School of Medicine, University of Maryland at Baltimore, 660 West Redwood Street, Baltimore, MD 21201.

METHODS

Samples

White rabbit (REG) and human (HEG) erythrocyte ghosts were obtained by hypotonic lysis as follows. Rabbit whole blood (10 ml) was collected by venipuncture into 0.3 ml of 1 M sodium citrate and washed in cold (0–4°C) isotonic phosphate (NaPi) buffer (32 ml, pH 7.4) by centrifugation (1,200 *g*, 10 min). All subsequent operations were also at 0–4°C. Human whole blood was similarly washed in isotonic NaPi. The buffy coat and supernatant were removed and the pellet resuspended with 32 ml of 5 mM NaPi buffer (pH 8.5) to cause hemolysis. After 20 min, the suspension was centrifuged (10,000 *g*, 20 min) followed by removal of the supernatant and resuspension with 20 mM

0006-3495/92/06/1557/13 $2.00

NaPi (pH 8.5) and centrifuged again into a pellet. Ghost membrane labeling was accomplished using 0.05 ml of ethanol containing 1,1'-dihexadecyl-3,3,3',3'-tetramethylindocarbocyanine perchlorate (DiI), at a concentration of 3.5 mg/ml, and adding this ethanol to a suspension made from the pellet which had a volume of 4.45 ml. The DiI was from Molecular Probes, Inc. (Eugene, OR). Before experiments ghost suspensions were resuspended and then mixed and diluted in the 20 mM NaPi buffer (pH 8.5) to obtain a concentration $\sim 3 \times 10^8$ ghosts/ml with 2% being labeled. The average rabbit and human erythrocyte ghost diameters are 5.8 and 6.5 μm (±5%), respectively (Bessis, 1973; Schalm et al., 1975).

Fusion chamber

All experiments were conducted using the two electrode fusion chamber shown in Fig. 1. The one-piece intermediate Parafilm (American Can Co., Greenwich, CT) layer, as shown, results in less drift of ghosts in suspension during experiments (which can interfere with counting ghosts during measurements) than with the chamber design previously described (Sowers, 1984).

Pulse generators

The electric circuit used to supply both the alternating current for inducing dielectrophoresis and the exponentially decaying fusogenic pulse was described previously (Sowers, 1989*a*). The exponential pulse was generated with a simple capacitor-discharge circuit and had adjustable decay half-time, t_e (ranging over ~0.1–4.6 ms), and peak voltage (up to 2.0 kV). A similar circuit was used to supply the square waveform fusogenic pulse. The square wave generator was developed at the A. N. Frumkin Institute of Electrochemistry in Moscow for preparative cell electrofusion and transfection protocols and could deliver a single pulse with widths, t_s, from 10 to 100 μs in discrete 10-μs steps, and from 100 to 1,000 μs in 100-μs steps, and amplitudes from 500 to 1500 V in 100-V steps. This was done by charging a 20-μF capacitor to a known voltage, then connecting it with the fusion chamber (which had an effective load resistance of ~1 kΩ with our buffer) by means of a high current pulse thyristor. At a known time after this connection was made, a second thyristor was connected the capacitor to a 3-Ω resistor thereby shunting the chamber. Thus a semisquare signal was actually formed by two intersecting exponentially decaying curves with decay times ~20 μF × ~1 kΩ (chamber resistance) ~20 ms and ~20μF × 3Ω (shunt resistance) = ~60 μs. The pulse length is defined as the point where the two decay curves intersect.

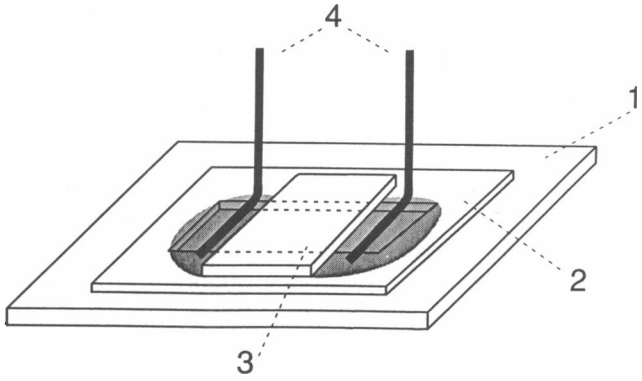

FIGURE 1 Fusion chamber design. A standard (22 × 22 mm, no. 1 thickness) microscope cover glass is used as the chamber base (*1*). The small Parafilm piece (12 × 12 mm) with a rectangular (1 × 8 mm) window (*2*) as well as the calibrated (3(±0.1) × 8 mm) coverslip (*3*) cut from a standard (25 × 75 mm) glass microscope slide were attached to the base by heating for 2–3 min at temperature sufficient to melt the Parafilm. When the chamber is attached with Scotch tape to the plastic (25 × 75 mm) slide support (not shown on the figure) with a square (13 × 13 mm) well, two wire spring electrodes (*4*) made of solder-tinned no. 22 gauge copper hook-up wire are pressed on both sides of the coverslip.

Protocols

Ghosts were placed into the fusion chamber (Fig. 1) by adding ~5 μl of ghost suspension at one end of the chamber to fill its working zone (i.e., the space of 0.1 × 1 × 3 mm^3 between the coverslip and the glass base). An additional ~5 μl of ghost suspension was added at the other end to make electrical continuity with the electrodes.

The fusion chamber containing the ghost suspension was placed on the table of an inverted fluorescence microscope. Ghost membranes were brought into close contact through dielectrophoresis-induced "pearl" chain formation. A sine wave current (60 Hz), applied to the electrodes, generated a field strength of 24 V (peak to peak)/mm in the chamber. After alignment was complete (1.5 min), a single (unless otherwise specified) high-voltage square or exponential pulse was applied. After an additional 1.5 min the fusion yield was determined.

Unless otherwise specified, all experiments were performed in 20 mM NaPi at 20–23°C. Other temperatures, over the range 2–37°C, were obtained by using a flow of dry ice-cooled air which then passed over an electric heater to an air jacket surrounding the fusion chamber. Temperature was controlled within ±1°C using a digital thermometer and manual adjustment of electric power to the resistors.

Membrane modifications

In some experiments the REG spectrin network was disrupted by heating at 42°C for 10 min before electrofusion (Chernomordik and Sowers, 1991). In other experiments the lipid matrix of REG was stabilized by 10^{-4} to 10^{-3} M uranyl acetate (Chizmadzhev and Abidor, 1980).

Measurements and data processing

Fusion yield. The efficiency of electrofusion was characterized by fusion yield, F, defined as a percentage of all ghosts which are fused:

$$F = \frac{N_f}{N_0} \times 100\% \quad (1)$$

where N_f is the number of originally labeled ghosts fused in the electrofusion process and N_0 is the total number of labeled ghosts in the sample volume before fusion. To find F, two methods were used.

Method 1. Values of F were calculated from the count of those events in a microscope sample area in which the fluorescent label moved (by lateral diffusion) from a labeled ghost to at least one adjacent but originally unlabeled neighbor in the same "Pearl" chain (Sowers, 1984). If the fusion yield is < ~60% such fluorescent chains are short and include two to five ghosts from which only one is orginally labeled. In this case fusion of a labeled ghost is displayed by a single fluorescent chain.

Method 2. Values of F were calculated by counting the number, N_{uf}, of the labeled ghosts which remained unfused after pulse. In this case

$$F = \left(1 - \frac{N_{uf}}{N_0}\right) \times 100\% \quad (2)$$

Both methods give the same results in the range of 10–60% (data not shown). However, method 1 is more convenient at lower F; method 2 is more convenient at higher F.

Values of N_0, N_f, and N_{uf} were determined by directly counting all labeled ghosts in the microscope field of view. Usually the concentration of labeled ghosts in the suspension was adjusted to obtain $N_0 \approx 100$. A mask placed in one of the microscope oculars to reduce the field of view by a factor of ~5 kept the ghost population from being too large to count. At least five measurements were made at different points around the center of the chamber. To find the average values of N_0, N_f, or N_{uf}, at least four chambers were examined. The values of N_0, N_{uf}, or N_f may vary over the range ±20% for different samples. To reduce errors (to ~10%) every set of experiments was performed with the same preparation of ghost.

Original values of N_0, N_{uf}, or N_f for rabbit and human erythrocyte ghosts were used to find F as a function of the pulse duration t_s (for square waveform) or t_e (for exponentially decaying pulses), electric field E_0, and temperature. These data were plotted in coordinates log(100-F) vs. t_s or t_e. In terms of the first-order kinetics theory (see Appendix I, Eqs. A-6 and A-8) the slopes of these plots give rate constants of the cell membrane electrofusion process.

Length-distributions of labeled fusion products (LFP)

Numbers N_n of LFP with a given number of contiguously labeled ghosts, n, were found by directly counting at least 100 LFP in each of four or five chambers. Then the average probabilities of labeled n-ghost chains formation were found as:

$$P_n = \frac{N_n}{N_c} \quad (3)$$

where N_c is the total number of LFP including unfused (single) labeled ghosts ($n = 1$) and contiguously labeled chains ($n > 1$). These values of P_n were compared with theoretical distributions calculated by means Eq. A-12.

RESULTS

Effect of pulse parameters on fusion yields

The fusion yield, F, as function of the strength, E_0, width, t_s, and total duration, Σt_s, of the square waveform pulses for two different REG preparations is shown in Figs. 2 *a* and 3*a*. As can be seen, F increases with both E_0 and t_s. However, the initial parts of the $F(t_s)$ curves show a slow increase in fusion yield at lower electric fields (E_0 = 1.7 and 2.0 kV/cm). This slow increase actually disappears at 3.0 kV/cm. Within the experimental error, application of several (from two to four) pulses (10 s between pulses) with a total duration Σt_s gives the same fusion yield as one pulse of the same duration (Fig. 3 *a*).

$F(t_s)$ curves for the HEG (Fig. 4 *a*) are similar to those for the REG. However for the same fusion yield the HEG require a relatively longer pulse duration or higher pulse strength E_0.

Results obtained for fusion of the REG and HEG using exponentially-decaying pulses (Fig. 5 *a*) are qualitatively similar to those for square waveform pulses (Figs. 2 *a* to 4 *a*). The quantitative difference is that a higher fusion yield is induced by the square waveform pulse than an exponential pulse with the same E_0 and $t_s = t_e$.

Figs. 2 *b* to 5 *b* show data for the REG and HEG plotted as log (100-F) vs. t_s or t_e. The straight lines were fitted to the experimental points by linear regression (in all cases the coefficient of variation was >0.97). Within

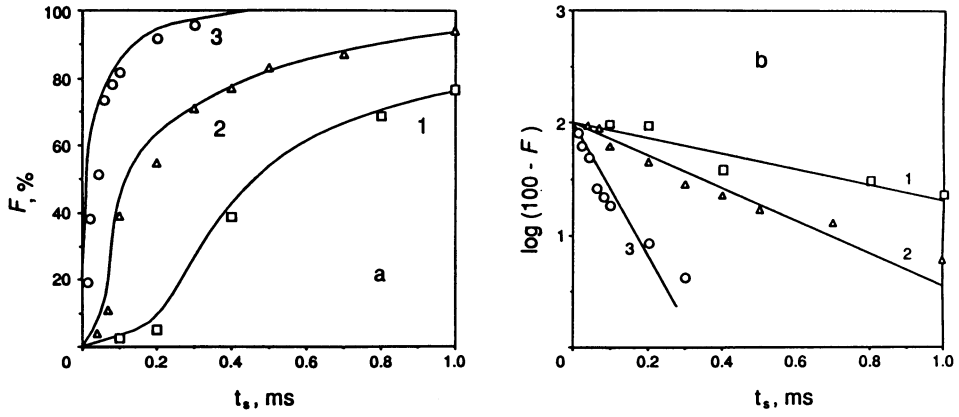

FIGURE 2 (*a*) Fusion yield of rabbit erythrocyte ghosts as a function of the square pulse width t_s for E_0 = 2.0 (curve 1), 2.3 (curve 2) and 3.kV/cm (curve 3). (*b*) The same data in a linear form according to Eq. A-5.

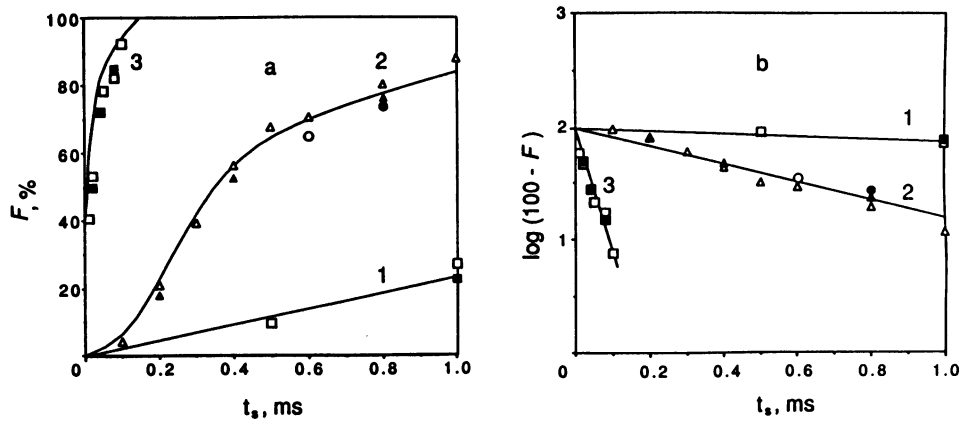

FIGURE 3 (*a*) Fusion yield of rabbit erythrocyte ghosts as a function of the total duration of square pulses Σt_s for $E_0 = 1.7$ (curve 1: [□] one pulse, [■] two pulses), 2.0 (curve 2: [△] one pulse, [▲] two pulses, [○] three pulses, [●] four pulses), and 3.0 kV/cm (curve 3: [□] one pulse, [■] two pulses). (*b*) The same data in a linear form.

experimental error all of these plots are linear. As follows from Eqs. A-5 and A-7 their slopes are proportional to the true (k_f) or effective (k_{ef}) fusion rate constants (see Appendix I).

Effect of the field strength on fusion rate constants

Values of k_f and k_{ef} (obtained from the slopes of log (100-F) vs. t_s or t_e plots) increase considerably with E_0 for both the REG and HEG (Fig. 6). Effective constants, k_{ef}, for the exponentially-decaying pulses are clearly much less than true constants, k_f, for the square waveform pulses (compare curves 1 and 2). Also, it should be noted that rate constants are notably larger for the REG than for the HEG (compare curves 1 and 3).

Effect of heat treatment at 42°C and exposure to uranyl ions

Modification of the REG by heating at 42°C for 10 min to disrupt the spectrin network (Chernomordik and Sowers, 1991) or exposure to 0.1–1.0 mM uranyl ions to stabilize membrane lipid matrix (Chizmadzhev and Abidor, 1980) leads to a decrease in the fusion yields (Fig. 7). However, the $F(t_s)$ data can still be put into linear semilog plots. Actually both treatments lead to a decrease in the fusion rate constant.

Temperature dependence of fusion rate constants

Fig. 8 shows the temperature dependence of the REG fusion rate constants as Arrhenius plots (lnk_f vs. recipro-

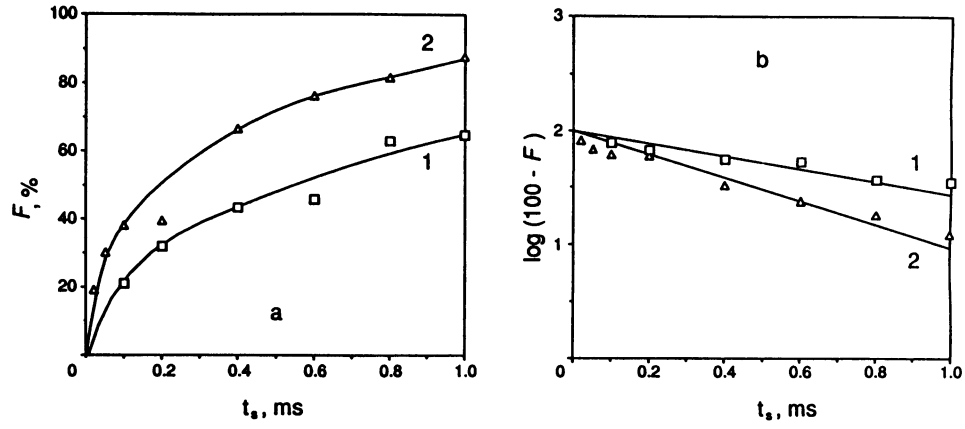

FIGURE 4 (*a*) Fusion yield of human erythrocyte ghosts as a function of the square pulse width t_s for $E_0 = 3.3$ (curve 1) and 5.0 kV/cm (curve 2). (*b*) The same data in a linear form.

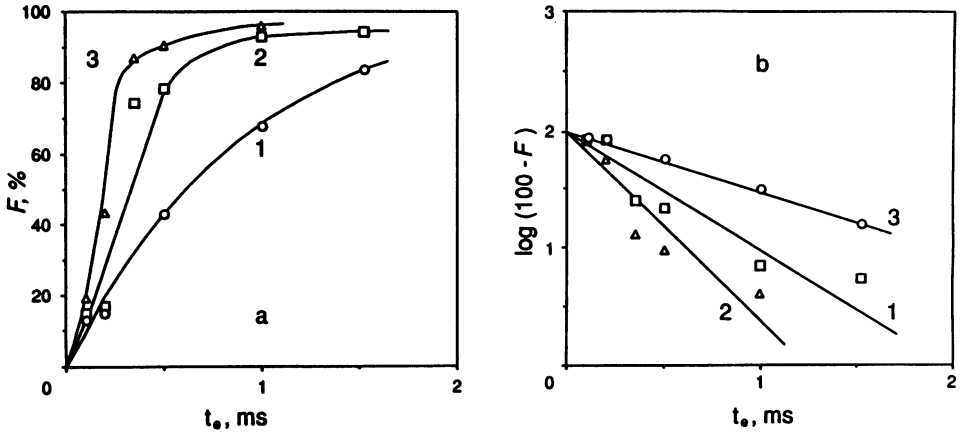

FIGURE 5 (*a*) Fusion yield of rabbit (curves 1 and 2) and human erythrocyte ghosts (curve 3) as a function of the decay half-time of exponential pulses t_e for E_0 = 3.5 (curve 1), 4.0 (curve 2), and 5.0 V/cm (curve 3). (*b*) The same data in a linear form according to Eq. A-7.

cal temperature °K, $1/T$) for E_0 = 2.3, 3.0, 3.7, and 5.0 kV/cm. As can be seen, all of these plots are linear which is typical for activated processes described by first-order rate kinetics. Slopes of these plots give the values of the activation energy E_a: 9.6, 6.8, 6.4, and 9.7 kT, respectively (where k is the Boltzmann constant).

Statistics of LFP

Length-distributions of LFP (Appendix II) obtained for REG with different pulses are shown in Figs. 9 and 10. It can be seen that an increase in the field strength or width leads to a widening of the distribution and a decrease in the yield, P_n, for short LFP. The probabilities, p, that a given membrane contact is fused was found from the experimental data using Eq. A-14. There is no obvious systematic trend in Fig. 9 *a'–c'* and thus p is actually independent of the chain length (i.e., n). However, the longer the LFP chain the more originally unlabeled ghosts it contains. The fact that p is the same for unfused (n = 1) ghosts and two-ghost chains (n = 2) as for long (n > 2) chains suggests that presence of the DiI label in the ghosts has no effect on their fusibility. Mean values of p, however, are strongly affected by pulse parameters. Values of P_n calculated with mean p, estimated as shown in Fig. 9 *a'–c'*, are in a good agreement with experimental data (Figs. 9 and 10).

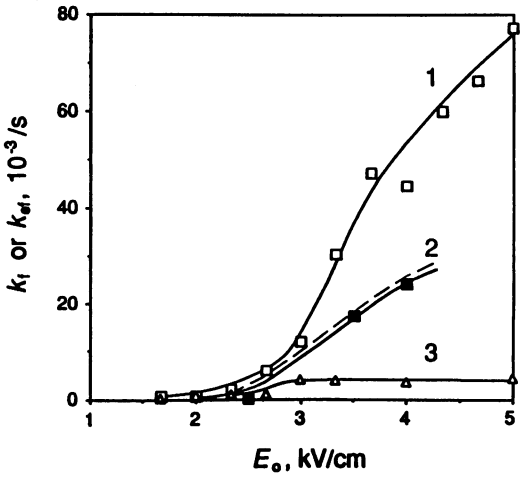

FIGURE 6 Fusion rate constants, k_f, as a function of the square (curves 1 and 3) and exponentially decaying (curve 2) waveform pulse field strength, E_0, for rabbit (curves 1 and 2) and human (curve 3) erythrocyte ghosts. Dashed line: the dependence of k_{ef} on t_e as calculated from curve 1 by numeric integration according to Eq. A-8.

DISCUSSION

Possible mechanisms of electrofusion

The purposes of this study were to better understand (*a*) the kinetics and (*b*) the mechanism of electrofusion. A priori three possible electrofusion mechanisms, with the electric field playing a different role in each, may be assumed.

1. A "trigger" mechanism: the fusion process is initiated by the electric field pulse but then proceeds without any further involvement of the field.
2. A "forced-based" mechanism: the fusion process is continuously "propelled" by the fusogenic electric field.
3. A "stochastic" mechanism: the electric field increases the probability of membrane fusion.

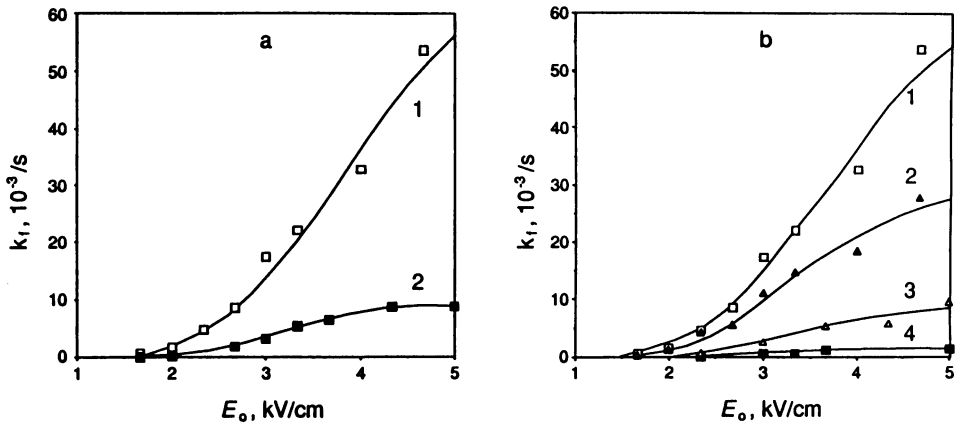

FIGURE 7 Effect of (*a*) heating (42°C, 10 min) and (*b*) uranyl ions on the field strength dependence of the REG fusion rate constants: (*a*) curve 1—control, curve 2—heating; (*b*) curve 1—0 (control), curve 2—10^{-4}, curve 3—$3 \cdot 10^{-4}$, curve 4—10^{-3} M uranyl acetate.

These three mechanisms would be expected to show essentially different phenomenology.

The trigger mechanism, actually favored by Teissei and Rols (1986) and Teissie et al. (1989), would relate electrofusion with the induction in the membranes of the so-called long-lived fusogenic state (Sowers, 1986, 1987, 1989*a*; Tsoneva et al., 1988). Generally, a trigger mechanism would be expected for an "all or nothing" type process which is initiated only when a stimulating factor (e.g., electric field) exceeds some "critical value" (e.g., a field threshold). However, earlier studies (Abidor et al., 1989; Sowers, 1989*a*) as well as data presented here show that the same values of fusion yield could be obtained with short but strong as well as weak but longer pulses. Thus there is no distinct "field threshold" in the electrofusion process and the pure trigger mechanism is rather unlikely.

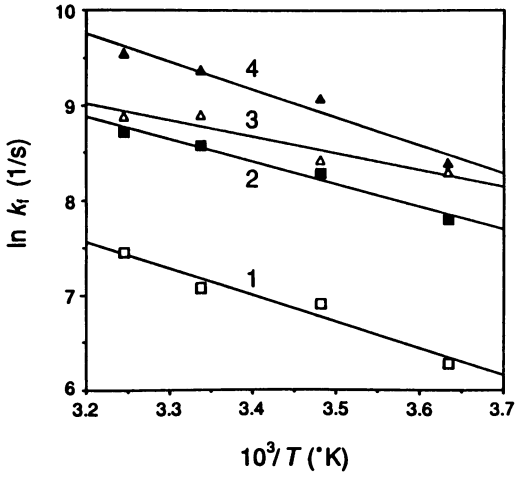

FIGURE 8 Arrhenius plots for the REG fusion rate constants at E_0 = 2.3 (curve 1), 3.0 (curve 2), and 3.7 (curve 3), and 5.0 kV/cm (curve 4).

The force-based electrofusion mechanism provides for a fusion process, which is driven by an electric force f_e which causes movement against friction in a viscous medium (the external water solution or the membrane itself as characterized by the viscosity η). This process requires time $t_f \sim \eta/f_e$ for completion. If the membrane system is homogeneous all fusion events would be synchronized by the fusogenic pulse. In this case one may expect a "time threshold" depending on the fusogenic electric field. However the experimental curves presented in Figs. 2 *a* to 5 *a* have no signs of the "time threshold" and therefore the forced movement is unlikely to be a primary factor of electrofusion.

An erythrocyte ghost suspension with a fraction of the ghosts carrying a membrane label is a very convenient system to study electrofusion as a stochastic process. In this system fusion of labeled ghosts with adjacent unlabeled neighbors is identified by the appearance of labeled chains independently of each other. That the electrofusion is a stochastic process is confirmed by results of the statistical study of the fusion product length distributions presented in Figs. 9 and 10. The stochastic character of electrofusion is presumed below.

Kinetics of electrofusion

For kinetic analysis the unlabeled ghosts may be considered as a background in which, upon fusion, the label moves laterally from single labeled ghosts to originally unlabeled but adjacent ghosts in the pearl chains. Under such conditions electrofusion may be formally described by first-order kinetics (Appendix I), which has been applied to a variety of processes such as radioactive

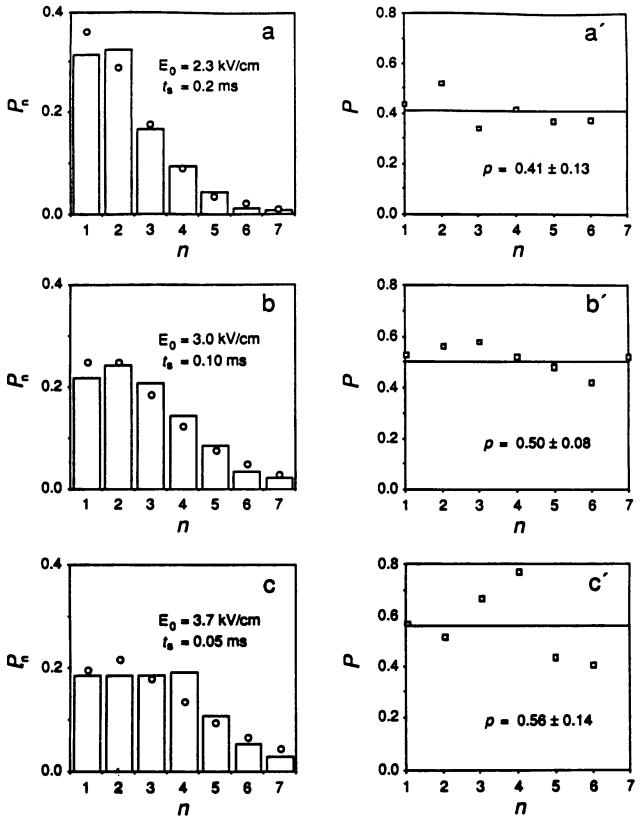

FIGURE 9 (*a–c*) Statistics of labeled fusion products for the rabbit erythrocyte ghosts treated by different fusogenic pulses: columns, experimental data; points, values calculated from Eq. A-12. (*a′–c′*) Probability of a fusion event (fusion of two given membranes) as function of number of ghosts in labeled fused chains: points are values calculated from experimental distributions using Eq. A-14; lines show mean p used to calculate P_n for corresponding points shown in *a–c*.

decay, bacterial growth, and chemical reactions. Although these processes are quite different the feature that they have in common is that the behavior of individual particles is probabilistic and independent of other identical particles or time.

As can be seen from Figs. 2 *b* to 5 *b*, fusion yield data for the REG and HEG fall on straight lines which are based on the first-order rate kinetics (Eqs. A-5 and A-7). Deviations from this kinetic behavior were observed for short low-field pulses (E_0 = 2 kV/cm) in the 0.2-ms range of pulse widths (Figs. 2 *a* and 3 *a*). This shows that electrofusion could be a more complicated process and may include more than one step. Otherwise the first-order rate kinetics always predominates under our experimental conditions and it can be accepted as a first approximation. Additional analysis is beyond the scope of this article.

The agreement of Eq. A-7 with experimental data for the exponential pulses gives additional support to the first-order rate kinetics. To derive this equation required that it be assumed that the fusion rate constant is dependent on the electric field. Although this dependence is unknown, it was possible to obtain Eq. A-7 in a form similar to Eq. A-5 and thus to relate the square waveform pulse data with the exponential waveform pulse data. As can be seen from Fig. 6 (curve 2), values of k_{ef}, calculated from k_f (dashed line) and found directly from experimental data for the exponentially decaying pulses (solid line), are very close.

Since the variable parameter in this kinetic description is the duration (i.e., t_s or t_e) of the fusogenic pulse, the agreement between experiment and theory indicates that the ghosts actually fuse (or start to fuse) only during rather than after the pulse. It does not mean that the fusion process stops occurring immediately after the pulse. However, later events, e.g., expansion of fusion lumens (Chernomordik and Sowers, 1991) or lateral diffusion of DiI, do not affect the fusion yield.

Fusion rate constants and related parameters

Depending on the experimental and theoretical approach, first-order rate processes can be described in different ways. The rate constant, k, is commonly used in chemical kinetics. For fast relaxation processes the parameter of choice is usually the mean lifetime, t_m. In the case of a bilayer lipid membrane (Abidor et al., 1979) this is the time interval that must pass before a given electric field induces, on the average, an irreversible damage or rupture of the membrane. In the process such as radioactive decay the half-time, T_h, is in common use. These parameters are related as follows (e.g., Marshal, 1978):

$$k = \frac{1}{t_f} = \frac{\ln 2}{T_h} \tag{4}$$

The fusion rate constant, which can be found directly from experimental data, has been used in this paper as a more convenient characteristic of electrofusion. However because (*a*) electrofusion is induced by short electric pulses, and (*b*) the most important part of this process proceeds only in the presence of the electric field, the mean fusion lifetimes t_f (i.e., the time interval during which ghosts remain unfused in the fusogenic electric field) may also be significant. Fig. 11 shows dependencies of t_f on E_0 for the rabbit and human erythrocyte ghosts as calculated from the k_f data. As can be seen, fusion lifetimes are short (from tens of microseconds to several milliseconds) and drastically decrease with E_0. This is similar to the behavior of artificial and cell membranes during irreversible electric breakdown (Abidor et al., 1979; Chernomordik et al., 1987).

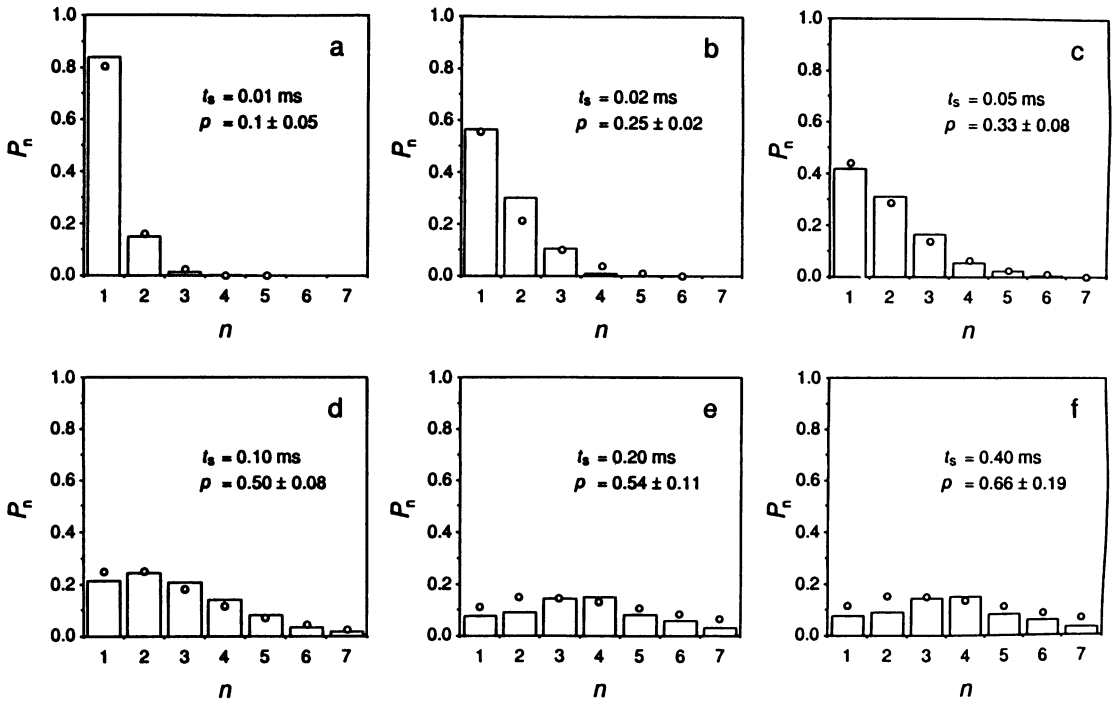

FIGURE 10 Statistics of labeled fusion products for the rabbit erythrocyte ghosts treated with 3.0-kV/cm square pulses of different t_s: columns, experimental data; open circles, values calculated as in Fig. 9.

The fusion rate constants are also related to the probability that a pair of membranes in contact become fused during the fusogenic pulse. According to Eqs. 3, A-5, A-7, and A-9:

$$p = 1 - \exp(-k_f t_s/2) \quad (5)$$

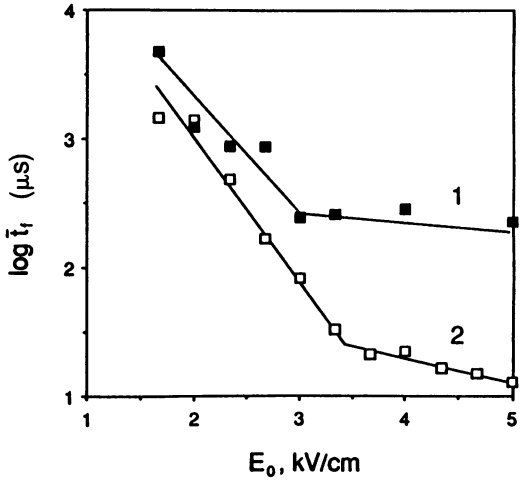

FIGURE 11 Fusion mean lifetime t_f of the rabbit (curve 1) and human (curve 2) erythrocyte ghosts as function of E_0.

A similar expression can be obtained for the exponentially-decaying waveform pulses. Note that Eq. 5 includes the product of the pulse width, t_s, and the fusion rate constant, k_f. The fusion rate constant, in turn, is a function of the field strength. Thus there is a reciprocity between t_s and E_0. This means that not only the same values of p, but also the length-distribution of fusion products, can be obtained with square (or exponentially decaying) waveform pulses having different parameters.

Fusion rate constants and the mechanism of cell membrane electrofusion

Because electrofusion can be induced regardless of the type of cells, it is possible to consider the initial stage of electrofusion as an essentially nonspecific physical process largely, but not completely (Sowers, 1989*b*), independent of the nature of cell membranes or metabolism (Zimmermann, 1982; Kuzmin et al., 1988; Abidor et al., 1989). Since the bilayer lipid matrix is structurally similar in all cell membranes, it rather than the membrane protein components is assumed to play the main role.

Generally fusion of lipid bilayers is prevented by strong steric electric and hydration forces (for review

see, e.g., Blumenthal, 1987; Wilschut and Hoekstra, 1991) and the membrane fusion process should involve local events, at least at the beginning (Hui et al., 1981; Sowers, 1989*a*; Kuzmin et al., 1988; Coackley and Gallez, 1989). It could be expected (Melikyan and Chernomordik, 1989) that cell membrane electrofusion starts from thin lipid bridges (stalks) formed between cell membranes in contact (Chernomordik et al., 1985) with further formation of intermediate trilaminar structures (Melikyan et al., 1982; Melikyan and Chernomordik, 1989). This mechanism, however, is unlikely for cell membrane electrofusion because the formation of stalks between lipid bilayers is expected only for some lipids with a negative spontaneous curvature (e.g., phosphatidylethanolamines). However, this contradicts the above-mentioned nonspecific character of electrofusion. Furthermore, the trilaminar structures have not been observed in EM pictures of electrofusion products (Stenger and Hui, 1986, 1989).

It has been reported (Sowers, 1986, 1987, 1989*a*, Teissie and Rols, 1986) that some cells can be fused even if the electric pulse is applied before, rather than after, the membranes are brought into contact. Hence, it was concluded that electric pulse-treated cells remain disposed to fuse upon contact at least many minutes after the pulse treatment. Up to now this long-lived fusogenic state has not been well studied (for review, see Sowers, 1989*a*). High electric field pulses induce other reversible long-lived effects including long-lived defects or pores (Sukharev et al., 1985; Sowers and Lieber, 1986) and permeabilization (Zimmermann, 1982; Serpersu et al., 1985; Neumann, 1989; Rols and Teissie, 1990), in cell membranes. Some authors consider the long-lived fusogenic state to be caused by electropermeabilization of cell membranes (Rols and Teissie, 1990) and suggest that this state could be the prime factor in the electrofusion process (Teissie et al., 1989). In an alternative viewpoint (Sowers, 1989*a*) electric field pulses may induce two independent processes: (*a*) electrofusion of cells already in contact (i.e., normal electrofusion) and (*b*) transition of cells into a special state similar, for example, to that for cells treated by chemical fusogens (Wilschut and Hoekstra, 1991). The first process is found to be much more effective and the importance of membrane contacts in the electrofusion process has been stressed by many authors (Sowers, 1989*a*; Sukharev et al., 1987, 1990; Abidor et al., 1989; Coackley and Galez, 1989).

It is known that electric pulses may induce a dramatic increase in cell membrane permeability due to reversible electric breakdown (Kinosita and Tsong, 1977; Benz et al., 1979; Chizmadzhev and Abidor, 1980), which is attributed to the induction of a large number of minute pores in the membrane lipid matrix. It is possible that reversible electric breakdown and electrofusion are phenomena unrelated with each other. In other words, the pulse may induce both measurable but otherwise separate effects: electroporation and electrofusion. Pilwat et al. (1981) were first to propose electropores as an intermediate stage on the path leading to electrofusion of adjacent cell membranes. This mechanism starts with the formation of pairs of coaxial pores filled by water and randomly positioned lipid molecules. The lipid molecules form bridges between the pores as minute "tubes" combining both membranes into a topologically single structure. Expansion of the membrane tubes then leads to mixing of cell contents which completes the fusion process. However, this mechanism has at least two vague points. First, it is not clear how lipid molecules can be pulled out of the lipid bilayer and, second, why they do not diffuse away instead of forming the "tube" bridges. However, the idea of combining coaxial pores was attractive to many authors (Dimitrov and Jain, 1984; Kuzmin et al., 1988; Pilwat et al., 1981; Zhelev et al., 1988; Zimmermann, 1982). Further development of the coaxial pore mechanism on a theoretical level by Kuzmin et al. (1988) suggested that the presence of the electric field may be important at all stages of the fusion process. Strong electric fields can (*a*) draw closely spaced membranes together, (*b*) promote the formation of coaxial pores, and (*c*) induce forces (owing to an electric current through coaxial pores) strong enough to push edges of the pores into contact and form the membrane tubes. Thus cell electrofusion may be directly related to reversible electric breakdown through coaxial pores induced in adjacent cell membranes in close contact.

In the following discussion, it will be assumed that the fusion rate constant, k_f, depends on the number of pores, m, created in each pair of membranes in contact. Actually k_f is the probability of transforming a pair of adjacent ghosts from the unfused state to the fused state. If fusion is a result of merging pores randomly scattered on both membranes in contact, k_f should be proportional to m^2. However pore formation in closely spaced membranes may be strongly correlated. Closely spaced membrane contacts of large area have a relatively high lateral electric resistance (Abidor et al., 1987) and the appearance of a pore in one membrane should, therefore, cause the transmembrane potential in the pore vicinity, but across the other membrane, to become doubled. This increases the probability of coaxial pore formation in the second membrane. Then it is more likely that $k_f \sim m$.

On the other hand, the number of pores m created during reversible electric breakdown should be proportional to the pore formation rate constant k_p. Hence:

$$k_f \sim k_p \tag{6}$$

The dependence of k_p on the electric field can be expressed (Glaser et al., 1988) as:

$$k_p = k_p(0)\exp(B\varphi^2) \tag{7}$$

or

$$\ln k_p = A_p + B\varphi^2 \tag{8}$$

where φ is the voltage drop across the membranes or the transmembrane potential, $k_p(0) = k_p$ at $\varphi = 0$, $A_p = \ln k_p(0)$, and B is a constant (of order of $\sim 4.8\ V^2$) given by the equation:

$$B = \frac{\pi r_*^2 \epsilon \epsilon_0}{2hkT} \tag{9}$$

where $r_* \approx 4$ Å is a critical radius above which originally hydrophobic pores become hydrophilic; h is the membrane thickness; ϵ and ϵ_0 are the dielectric constants of vacuum and water, respectively. Combining Eqs. 6 and 8 gives:

$$\ln k_f = A_f + B\varphi^2 \tag{10}$$

Thus we have found a functional dependence of the fusion rate constant on the fusogenic electric field. It shows that, in terms of the coaxial pore mechanism, the slope of the $\ln k_f$ vs. φ^2 curves should equal B. Demonstrating this experimentally requires an estimation of the membrane potentials, φ, created by the electric field pulse.

The maximal transmembrane potential induced by an external electric field in randomly suspended spherical-shaped cells is at the "cell poles," and is estimated (e.g., Kinosita and Tsong, 1977) as:

$$\varphi = \frac{3}{2}ER \tag{11}$$

where R is the cell radius. However the distribution of an electric field around the "pearl chains" is expected to differ from that for ghosts in suspensions. In chains the ghosts are pressed toward each other by electric forces and tight contact zones are formed at the ghost poles. Such contacts can be treated as a series of membrane capacitors. Thus if a unit of chain length (1 cm) contains N_c ghosts, then:

$$\varphi = \frac{E}{2N_c} = ER \tag{12}$$

This is 1.5 times less than that for suspended ghosts. Actual values of φ should be between these two limits, and are more likely to be closer to the lower limit. Here, values of φ were calculated using Eq. 12.

As can be seen from Fig. 12, the $\ln k_f$ vs. φ^2 dependencies for the REG and HEG are similar. The initial parts

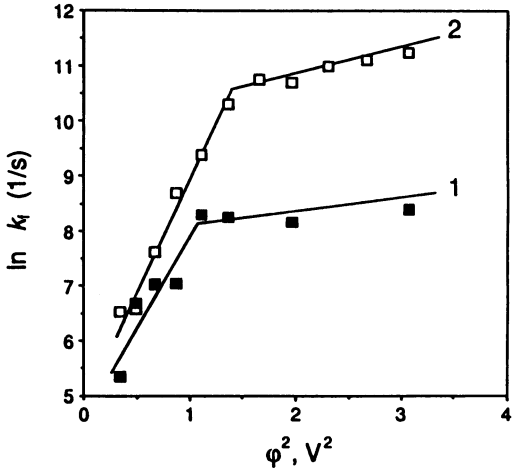

FIGURE 12 Plots of $\ln k_f$ vs. φ^2 for the rabbit (curve 1) and human (curve 2) erythrocyte ghosts.

of both plots are linear and their slopes are 4.2 and 3.3 V^{-2}, respectively. These values are close to $B = 4.8\ V^{-2}$ found both theoretically and experimentally for reversible electrical breakdown (Glaser et al., 1988). Moreover, as seen in Fig. 13, the initial slopes of the $\ln k_f$ vs. φ^2 plots actually do not change after heat treatment (42°C, 10 min) or in the presence of uranyl-ions. This is reasonable because B is expected to have a weak dependance on either the membrane cytoskeleton or the bilayer lipid structure in that Eq. 9 has no parameters that could significantly change B. On the other hand, the number of potential fusogenic sites (i.e., pores) could be different. This is why both heating and exposure to uranyl ions decrease the fusion yields without changing B.

Measurements of fusion yields at different temperatures give additional and independent evidence for the coaxial-pore model. Activation energies E_a, found from Arrhenius plots of the REG fusion rate constants, are in the range of 6–10 kT. These values need to be compared with activation energies for reversible formation of pores in high electric fields but such experimental data unfortunately are not available. However, by using Eq. 8, it is possible to estimate the difference of E_a for two transmembrane potentials, φ_1 and φ_2. Thus for fusion the REG at 2.3 and 3.0 kV/cm (φ_1 and φ_2 correspond to 0.82 and 1.05 V), $\Delta E_a = B\ (\varphi_1^2 - \varphi_2^2) = 4.8\ (0.82^2 - 1.05^2) \approx -2.1\ kT$, which is close to $\Delta E_a = 6.7\text{–}9.3 = -2.6\ kT$ corresponding to the experimental values of E_a. It should be noted that at relatively high induced transmembrane potentials (> 1.0 V) the fusion activation energy increases. This as well as the decrease in the slopes of the $\ln k_f$ vs φ^2 plots at high φ (to the right of the discontinuity in Figs. 12 and 13) may reflect some change in the electrofusion process. A similar effect was

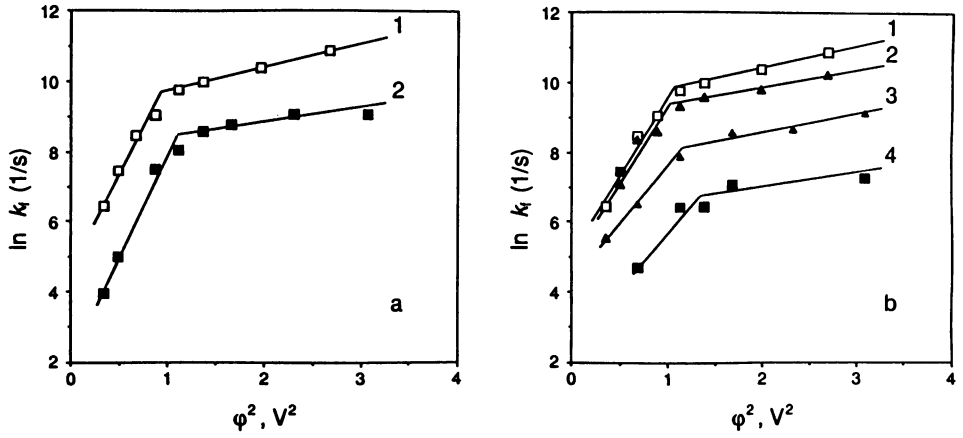

FIGURE 13 Plots of $\ln k_f$ vs. φ^2 for the rabbit erythrocyte ghosts (*a*) preheated at 42°C and (*b*) in presence of uranyl ions: (*a*) curve 1, control; curve 2, heating; (*b*) curve 1, 0; curve 2, 10^{-4}; curve 3, $3 \cdot 10^{-4}$; curve 4, 10^{-3} M uranyl acetate.

also observed in experiments on reversible electrical breakdown of bilayer lipid membranes (Glaser et al., 1988). Possibly in a high field the conductivity of membranes becomes so high that a considerable part of the electric field drops in the solution inside ghosts and the actual values of φ are much less than calculated values.

Thus the results of both kinetic analysis and statistical study indicate that (*a*) cell membrane electrofusion is a stochastic process proceeding only when a fusogenic electric field is applied to the membrane system, and (*b*) this process may be directly related to coaxial pores induced in the membranes owing to reversible electric breakdown.

APPENDIX I

Cell membrane electrofusion as a first-order rate process

In a fluorescence microscope a suspension of erythrocyte ghosts, some of which are DiI labeled, only fluorescent ghosts are visible as randomized separated bright spheres against a dark background. If ghosts have been brought into a close contact to form the "pearl chains" by means dielectrophoresis, then application of a fusogenic electric pulse may induce a fraction of the labeled ghosts to fuse with neighbors forming labeled chains as DiI laterally moves from labeled ghosts to adjacent originally unlabeled ghosts. A conversion of labeled ghosts from the unfused (G_{uf}) to the fused (G_f) state may be described as $G_{uf} \rightarrow G_f$. If, in any given "pearl chain," any fusion event is independent of other fusion events and if it is governed only by a pure chance, then the number of unfused labeled ghosts, n_{uf}, decreases with the rate given by:

$$\frac{dn_{uf}}{dt} = -k_f n_{uf} \qquad \text{(A-1)}$$

where t is time of the process and k_f is the fusion rate constant. Solving Eq. A-1 for cell membrane electrofusion requires two considerations: (*a*) the fusion rate constant should be a function of the electric field, E, since the fusion yield, F, is highly dependant on the pulse amplitude E_0, i.e., $k_f = k_f(E)$; and (*b*) the fusion assay involves counting fused or unfused cells at least 1.5 min after the electric pulse. Thus it is important to define t, i.e., to find out whether electrofusion occurs during or after the pulse treatment. If the electrofusion process proceeds only during the electric pulse of duration t_p, then $0 \le t \le t_p$ and Eq. A-1 can be transformed to:

$$\int_{N_0}^{N_{uf}} \frac{dn_{uf}}{n_{uf}} = -\int_0^t k_f(E)dt \qquad \text{(A-2)}$$

or

$$\ln \frac{N_{uf}}{N_0} = -\int_0^t k_f(E)dt \qquad \text{(A-3)}$$

where N_0 is the total number of labeled cells and N_{uf} is the number of unfused ghosts after electrofusion. Taking into account the definition of fusion yield, Eq. A-3 can be rewritten as:

$$\ln(100 - F) = -\int_0^t k_f(E)dt \qquad \text{(A-4)}$$

Further solution of this equation depends on whether the waveform is square or exponential.

Square pulses

In this case $t_p = t_s$ and, as long as the field strength equals E_0 and does not change during the pulse, k_f is a constant. Hence:

$$\log(100 - F) = 2 - 0.43 k_f t_s \qquad \text{(A-5)}$$

This expression is linear relative to t_s and the slope of the $\log(100 - F)$ vs. t_s dependence is proportional to the fusion rate constant k_f.

Exponential pulses

In the interval $0 \le t \le t_p = \infty$ the value of E decreases from E_0 to 0 as

$$E = E_0 \exp\left(-\frac{\ln 2t}{t_e}\right) \qquad \text{(A-6)}$$

In this case Eq. A-4 may be transformed to:

$$\log(100 - F) = 2 - 0.63k_{ef}t_e \quad \text{(A-7)}$$

where

$$k_{ef} = \int_0^\infty k_f(E_0 \exp(-x))dx \quad \text{(A-8)}$$

and $x = \ln 2 \cdot t/t_e$). Eq. A-7 is similar to Eq. A-5, but Eq. A-7 includes the effective constant k_{ef} and the pulse half-time t_e instead of k_f and t_s. It should be noted that, since Eq. A-8 is integrated over $0 \le x \le \infty$, k_{ef} does not depend on t_e and is defined only by E_0.

APPENDIX II

Length distribution of labeled fusion products (LFP)

When originally DiI-labeled ghosts fuse with adjacent unlabeled ghosts, LFP of different length are formed. In our experimental system, the number of originally labeled ghosts is relatively small and any labeled chains formed in the electrofusion process are assumed to contain only one originally labeled ghost. Thus all LFP are assumed to have come about as a result of independent events.

In long (infinite) "pearl chains" each ghost has two neighbors, i.e., each one forms two membrane contacts. If p is the probability that at time t a given membrane contact has fused, then the probability of finding a given contact unfused is $1 - p$. It is now necessary to find the probability P_n that a labeled chain selected at random contains exactly n ghosts.

The chance that a given labeled ghost remains unfused after application the fusogenic electric pulse is the product of the probabilities that the ghost does not fuse with either of its two neighbors in the same "pearl chain," that is:

$$P_1 = (1 - p)^2 \quad \text{(A-9)}$$

The probability that a given labeled ghost will fuse with a given neighbor is $p(1 - p)^2$ because the fusion process involves simultaneously three events: the first is fusion at the contact between the labeled and unlabeled ghosts with the probability of p, and two others are the absence of fusion at contacts of these ghosts with other ones with the probabilities $1 - p$. The probability of formation of chains containing two ghosts is actually two times higher because to form a two-ghost chain a labeled ghost can fuse with any of its two neighbors, thus

$$P_2 = 2p(1 - p)^2 \quad \text{(A-10)}$$

The formation of a labeled three-ghost chain containing an originally labeled ghost in a certain position involves two fusion events and two nonfusions on the chain ends and had a chance of $p^2(1 - p)^2$. Because in a three-ghost chain the originally labeled ghost can occupy three different positions (i.e., either of ends or the center), the probability finding such a chain is three times higher, i.e.:

$$P_3 = 3p^2(1 - p)^2 \quad \text{(A-11)}$$

Generally, for chains containing n fused ghosts from which only one was originally labeled, the probability is:

$$P_n = np^{n-1}(1 - p)^2 \quad \text{(A-12)}$$

This satisfies the obvious condition:

$$\sum_{n=1}^{\infty} P_n = 1 \quad \text{(A-13)}$$

From Eq. A-12 it also follows:

$$p = (n - 1)P_n/nP_{n-1} \quad \text{(A-14)}$$

Ms. Myong Soon Cho is gratefully acknowledged for expert technical assistance. Support from ONR grant N00014-92-J-1053 to Dr. Sowers.

Received for publication 30 May 1991 and in final form 4 February 1992.

REFERENCES

Abidor, I. G., V. B. Arakelyan, L. V. Chernomordik, Yu. A. Chizmadzhev, V. F. Pastushenko, and M. R. Tarasevich. 1979. Electrical breakdown of bilayer lipid membranes. *Bioelectrochem. Bioenerg.* 6:37–52.

Abidor, I. G., A. I. Barbul, D. Zhelev, S. I. Sukharev, P. I. Kuzmin, V. F. Pastushenko, and A. V. Zelenin. 1989. Electrofusion and electrical properties of cell pellets in centrifuge. *Biol. Membr.* 12:212–224. (In Russian.)

Abidor, I. G., V. F. Pastushenko, E. M. Osipova, G. B. Melikyan, P. I. Kuzmin, and S. V. Fedotov. 1987. Relaxation studies of the plane contact of bilayer lipid membranes. *Biol. Membr.* 4:67–76. (In Russian.)

Benz, R. F., F. Beckers, and U. Zimmerman. 1979. Reversible electrical breakdown of lipid bilayer membranes: a charge-pulse relaxation study. *J. Membr. Biol.* 48:181–204.

Bessis, M. 1973. Living Blood Cells and Their Ultrastructure. Springer-Verlag, Inc., New York. 767 pp.

Blumenthal, R. 1987. Membrane fusion. *Curr. Top. Membr. Transp.* 29:203–254.

Chernomordik, L. V., M. M. Kozlov, G. B. Melikyan, I. G. Abidor, V. S. Markin, and Yu. A. Chizmadzhev. 1985. The shape of lipid molecules and monolayer membrane fusion. *Biochim. Biophys. Acta.* 812:643–655.

Chernomordik, L. V., and A. E. Sowers. 1991. Evidence that the spectrin network and a nonosmotic force control the fusion product morphology in electrofused erythrocyte ghosts. *Biophys. J.* 60:1026–1037.

Chernomordik, L. V., S. I. Sukharev, S. V. Popov, V. F. Pastushenko, A. V. Sokirko I. G. Abidor, and Yu. A. Chizmadzhev. 1987. The electrical breakdown of cell and lipid membranes: the similarity of phenomenologies. *Biochim. Biophys. Acta.* 902:360–373.

Chizmadzhev, Yu. A., and I. G. Abidor. 1980. Membranes in strong electric fields. *Bioelectrochem. Bioenerg.* 7:83–100.

Coackley, W. T., and D. Gallez. 1989. Membrane-membrane contact: involvement of interfacial instability in the generation of discrete contacts. *Biosci. Rep.* 9:675–691.

Dimitrov, D. S., and R. K. Jain. 1984. Membrane stability. *Biochim. Biophys. Acta.* 779:437–468.

Glaser, R., S. L. Leikin, L. V. Chernomordik, A. V. Sokirko, and V. F. Pastushenko. 1988. *Biochim. Biophys. Acta.* 940:275–287.

Hui, S. W., T. P. Stewart, L. T. Boni, and P. L. Yeagle. 1981. Membrane fusion through point defects in bilayers. *Science* (*Wash. DC*). 212:921–922.

Kinosita, K., and T. Y. Tsong. 1977. Voltage-induced pore-formation and hemolysis of human erythrocytes. *Biochim. Biophys. Acta.* 471:227–242.

Kuzmin, P. I., V. F. Pastushenko, I. G. Abidor, S. I. Sukharev, A. I. Barbul, and Yu. A. Chizmadzhev. 1988. Theoretical analysis of a cell electrofusion mechanism. *Biol. Membr.* 5:600–612. (In Russian.)

Marshall, A. G. 1978. Biophysical Chemistry: Principles, Techniques, and Applications. J. Wiley & Sons, New York.

Melikyan, G. B., I. G. Abidor, L. V. Chernomordik, and L. M. Chailahyan. 1982. Electrostimulated fusion and fission of bilayer lipid membranes. *Dokl. Akad. Nauk. SSSR* 263:1009–1013. (In Russian.)

Melikyan, G. B., and L. V. Chernomordik. 1989. Electrofusion of lipid bilayers. *In* Electroporation and Electrofusion in Cell Biology. E. Neumann, A. E. Sowers, and C. Jordan, editors. Plenum Press, New York. 181–192.

Neumann, E. 1989. Relaxation Hysteresis of Membrane Electroporation. *In* Electroporation and Electrofusion in Cell Biology. E. Neumann, A. E. Sowers, and C. Jordan, editors. Plenum Press, New York. 61–82.

Neumann, E., A. E. Sowers, and C. Jordan, editors. 1989. Electroporation and Electrofusion in Cell Biology. Plenum Press, New York.

Pilwat, G., H.-P. Richter, and U. Zimmerman. 1981. Giant culture cells by electric-field induced fusion. *FEBS* (Fed. Eur. Biochem. Soc.) *Lett.* 133:169–174.

Pohl, H. A. 1978. Dielectrophoresis. Cambridge University Press, London.

Rolls, M. P., and J. Teissie. 1990. Electropermeabilization of mammalian cells-quantitative analysis of the phenomenon. *Biophys. J.* 58:1089–1098.

Schalm, O. W., Jain, N. C., and E. J. Carroll. 1975. Veterinary Hematology, 3rd editor. Lea & Febiger, Philadelphia.

Senda, M., J. Takeda, S. Abe, and T. Nakamura. 1979. Introduction of cell fusion of plant protoplasts by electrical stimulation. *Plant Cell Physiol.* 20:1141–1443.

Serpersu, E. H., K. Kinosita, Jr., and T. Y. Tsong. 1985. Reversible and irreversible modification of erythrocyte membranes permeability by electric field. *Biochim. Biophys. Acta.* 812:779–885.

Sowers, A. E. 1984. Characterization electric field-induced fusion in erythrocyte ghosts membranes. *J. Cell Biol.* 99:1989–1996.

Sowers, A. E. 1986. A long-lived fusogenic state is induced in erythrocyte ghosts by electric pulses. *J. Cell Biol.* 102:1358–1362.

Sowers, A. E. 1987. The long-lived fusogenic state induced in erythrocyte ghosts by electric pulses is not lateral mobile. *Biophys. J.* 52:1015–1020.

Sowers, A. E. 1989*a*. The mechanism of electroporation and electrofusion in erythrocyte membranes. *In* Electroporation and electrofusion in Cell Biology. E. Neumann, A. E. Sowers, and C. Jordan, editors. Plenum Press, New York. 229–256.

Sowers, A. E. 1989*b*. Evidence that electrofusion yield is controlled by biologically relevant factors. *Biochim. Biophys. Acta.* 985:334–338.

Sowers, A. E. 1992. Mechanisms of electroporation and electrofusion. *In* Guide to Electroporation and Electrofusion. D. C. Chang, B. M. Chassy, J. A. Saunders, and A. E. Sowers, editors, Academic press, Inc., San Diego. 119–138.

Sowers, A. E., and M. L. Lieber. 1986. Electropores in individual erythrocyte ghosts: diameters, lifetimes, numbers, and location. *FEBS* (*Fed. Eur. Biochem. Soc.*) *Lett.* 205:179–184.

Stenger, D. A., and S. W. Hui. 1986. Kinetics of ultrastructural changes during electrically-induced fusion of human erythrocytes. *J. Membrane Biol.* 93:43–53.

Stenger, D. A., and S. W. Hui. 1989. Electrofusion kinetics: studies using electron microscopy and fluorescence contents mixing. *In* Electroporation and Electrofusion in Cell Biology. E. Neumann, A. E. Sowers, and C. Jordan, editors. Plenum Press, New York. 167–180.

Sukharev, S. I., I. N. Bandrina, A. I. Barbul, I. G. Abidor, and A. V. Zelenin. 1987. Electrofusion of fibroblast-like cells. *Stud. Biophys.* 119:45–48.

Sukharev, S. I., I. N. Bandrina, A. I. Barbul, I. G. Abidor, and A. V. Zelenin. 1990. Electrofusion of fibroblasts on porous membrane. *Biochim. Biophys. Acta.* 1034:125–131.

Sukharev, S. I., L. V. Chernomordik, S. V. Popov, and I. G. Abidor. 1985. A patch-clamp study of electrical breakdown of cell membranes. *Biol. Membr.* 2:77–86. (In Russian.)

Teissie, J., and M. P. Rols. 1986. Fusion of mammalian cells in culture is obtained by creating the contact between cells after electropermeabilization. *Biochem. Biophys. Res. Commun.* 140:258–266.

Teissie, J., M. P. Rols, and C. Blangero. 1989. Electrofusion of mammalian cells and giant unilamellar vesicles. *In* Electroporation and Electrofusion in Cell Biology. E. Neumann, A. E. Sowers and C. Jordan, editors. Plenum Press, New York. 203–214.

Tsoneva, I., I. Panova, P. Doinov, D. S. Dimitrov, and D. Strahilov. 1988. Hybridoma production by electrofusion: monoclonal antibodies against the Hc antigene of Salmonella. *Stud. Biophys.* 125:31–35.

Wilschut, J., and D. Hoekstra. 1991. Membrane Fusion. Marcel Dekker, Inc., New York. 902 pp.

Zhelev, D. V., D. S. Dimitrov, and P. Doinov. 1988. Correlation between physical parameters in electrofusion and electroporation of protoplasts. *Bioelectrochem. Bioenerg.* 20:155–167.

Zimmermann, U. 1982. Electric field-mediated fusion and related electrical phenomena. *Biochim. Biophys. Acta.* 694:227–277.